

Realistic interpretation of quantum mechanics and encounter-delayed-choice experiment

GuiLu Long^{1,2,3*}, Wei Qin¹, Zhe Yang¹, and Jun-Lin Li¹¹State Key Laboratory of Low-Dimensional Quantum Physics and Department of Physics, Tsinghua University, Beijing 100084, China;²Innovative Center of Quantum Matter, Beijing 100084, China;³Tsinghua National Laboratory for Information Science and Technology, Tsinghua University, Beijing 100084, China

Received September 25, 2017; accepted October 19, 2017; published online December 13, 2017

In this paper, a realistic interpretation (REIN) of the wave function in quantum mechanics is briefly presented. We demonstrate that in the REIN, the wave function of a microscopic object is its real existence rather than a mere mathematical description. Specifically, the quantum object can exist in disjointed regions of space just as the wave function is distributed, travels at a finite speed, and collapses instantly upon a measurement. Furthermore, we analyze the single-photon interference in a Mach-Zehnder interferometer (MZI) using the REIN. Based on this, we propose and experimentally implement a generalized delayed-choice experiment, called the encounter-delayed-choice experiment, where the second beam splitter is decided whether or not to insert at the encounter of two sub-waves along the arms of the MZI. In such an experiment, the parts of the sub-waves, which do not travel through the beam splitter, show a particle nature, whereas the remaining parts interfere and thus show a wave nature. The predicted phenomenon is clearly demonstrated in the experiment, thus supporting the REIN idea.

wave function, realistic interpretation, Mach-Zehnder interferometer, wave-particle duality**PACS number(s):** 03.65.Ta, 03.65.Ud, 42.50.Xa, 42.50.Dv**Citation:** G. L. Long, W. Qin, Z. Yang, and J. L. Li, Realistic interpretation of quantum mechanics and encounter-delayed-choice experiment, *Sci. China-Phys. Mech. Astron.* **61**, 030311 (2018), <https://doi.org/10.1007/s11433-017-9122-2>

1 Introduction

The wave-particle duality is a central concept of quantum mechanics and has been strikingly illustrated in the well-known Wheeler's delayed-choice gedanken experiments [1-9]. A good demonstration of the delayed-choice experiments is given by a two-path interferometer, the Mach-Zehnder interferometer (MZI), shown in Figure 1(a). A single photon is directed to the MZI, which is followed by two detectors at its end. If the output beam splitter BS₂ is present (closed configuration), the photon is first split by the input beam splitter BS₁ and then travels inside the MZI with a tunable phase shifter ϕ until the two interfering paths are recombined by

BS₂. When ϕ is varied, the interference fringes are observed as a modulation of the detection probabilities of the detectors D₁ and D₂. This implies that the photon travels along both arms of the MZI and behaves as a wave. In this case, the two paths are indistinguishable. If BS₂ is absent (open configuration), a click in only one of the two detectors with probability 1/2, independent of ϕ , is associated with a given path, indicating that the photon travels along a single arm and behaves as a particle. Such an experiment concludes that quantum systems exhibit wave or particle behavior depending on the configuration of the measurement apparatus. Moreover, two complementary experimental setups are mutually exclusive and the two behaviors, wave and particle, cannot be observed simultaneously. Recently, a new extension of the delayed-

*Corresponding author (email: gllong@mail.tsinghua.edu.cn)

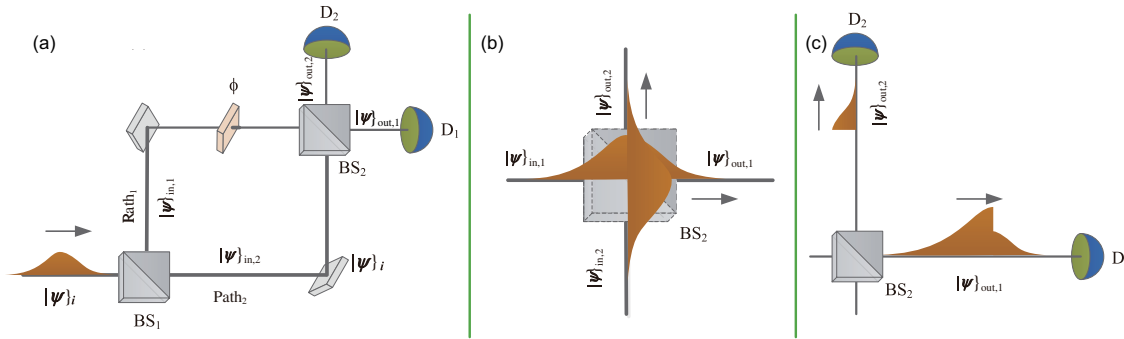


Figure 1 (Color online) (a) An MZI with a tunable phase ϕ between its two arms. In the delayed-choice MZI, the decision whether or not to insert BS_2 is made after the photon has entered the MZI, but has not arrived at the intended position of BS_2 (the exit point). (b) In the EDC experiment, the insertion of BS_2 is made right at the encounter of the two sub-waves. As shown here, the front parts of the sub-waves have passed the exit point and are “closed” by BS_2 . (c) Still in the EDC experiment, the two sub-waves leave the MZI and continue to move forward to D_1 and D_2 . The front parts of the sub-waves retain their shape before they leave the MZI, but the back parts of the sub-waves are changed by the inserted BS_2 . The back part of the up-going sub-wave vanishes due to destructive interference, whereas the right-going part of the sub-wave increases due to the constructive interference of BS_2 . The interference patterns of the back parts of the sub-waves may vary according to their relative phases.

choice experiment, called quantum delayed choice (QED) [10-19], where the classical state of the output beam splitter is replaced with a quantum superposition state, has been proposed and experimentally demonstrated. The experiment indicates that BS_2 can be simultaneously absent and present, such that both wave and particle behaviors can be simultaneously observed, indicating a morphing behavior between wave and particle.

The concept of a wave function is introduced to quantum theory, as a complete description of a quantum system. The wave function can be determined through tomographic methods, and even be directly measured by the sequential measurements of two complementary variables relying on a weak measurement [20-22]. It is the heart of quantum theory and its typical interpretation is provided by the Copenhagen interpretation [23], where the wave function is treated, in a pure mathematical manner, as a complex probability amplitude. Despite such efforts, the essential understanding of the wave function has not been solved so far [24, 25].

In this article, we propose a realistic interpretation (REIN) of the wave function in quantum mechanics, and then a generalized delayed-choice experiment, the encounter-delayed-choice (EDC) experiment to test the REIN. The EDC is experimentally demonstrated, and the results agree with the theoretical interpretation very well, thus supporting the idea of the REIN. In the following, we will first present the main points of the REIN. Then, we describe the EDC experiment proposal, followed by an experimental demonstration. Finally, we present the discussion and summary.

2 The realistic interpretation (REIN)

The essential idea of the REIN is that the wave function is the

realistic existence rather than just a mathematical description. Here we give a brief introduction, and a detailed description will be given elsewhere [26].

A quantum object, an object that obeys quantum mechanics, exists in the form of a wave function: extended in space and even in disjointed regions of space in some cases. Since being usually a complex function, the wave function usually has a amplitude and a phase. If we just look at its spatial distribution, the square of the modulus of the wave function gives the spatial distribution. It changes the form as the wave function changes frequently. However, it also has a phase, and when two sub-wave functions merge or have an encounter, the resulting wave function will change differently at different locations: some are strengthened due to constructive interference, whereas some others are canceled due to destructive interference. Thus, a photon in an MZI is an extended object that exists in both arms. In the REIN perspective, no difference exists between a photon in a closed MZI setting and that in an open setting before they arrive at the second beam splitter. It is also easier to comprehend how a photon can travel both arms. In the REIN, a photon is an extended and separated object that exists simultaneously at both arms, just like a water stream divided into two branches, each then flowing on its own riverbed. Certainly, the quantum wave function is more powerful than the water stream. This is because such a function has a phase factor that can cause the interference.

Given that a sub-wave function is a part of the whole wave function, for instance, the wave function in the upper arm of the MZI, it needs not to be normalized [27]. To emphasize, we use $|\psi\rangle$ and $\langle\psi|$ to denote a sub-wave function throughout this article.

The quantum wave function, the true or realistic quantum

object, moves at a speed that is less than or equal to the speed of light. As we know, light, an ensemble of photons, takes 8 min and 20 s to travel from the Sun to our planet. The electrons in a cyclotron travels at a speed slower than that of light when it is accelerated.

In addition, the quantum wave function, or a quantum object, can change the form by a transformation or by a measurement. Although visualizing the change in the wave function is easy, it is often difficult to visualize the change in a quantum object. This difficulty is pertinent to our stubborn notion of a rigid particle of microscopic object for a quantum object, as the name, “quantum particle” suggests. If we adopt the view that the quantum object does exist in the form of the wave function, it is easier to understand this form change. Hence, a photon wave function changes into two sub-wave functions when it is transformed by a beam splitter.

A measurement drastically changes the shape or form of a quantum object. According to the measurement postulate of quantum mechanics, a measurement collapses the wave function instantly into one of the eigenstate of the measured observable. This change of the quantum object takes no time, and it is within all the spaces occupied by the wave function, which are disjointed in some cases. The measurement postulate cannot be derived from the Schrödinger equation, which governs the evolution of the quantum wave function. At this stage, one should not ask why measurement has such dramatic effect. The quantum object simply behaves in this natural manner.

3 Encounter-delayed-choice (EDC) experimental proposal

According to the REIN, a single photon is considered as the whole spatial distribution of its wave function, which really exists, more than a mere mathematical description. A new interpretation of the single-photon interference experiment in the MZI is given in the REIN perspective. The action of a 50/50 beam splitter can be described by a so-called Hadamard transformation expressed as:

$$H = \frac{1}{\sqrt{2}} \begin{pmatrix} 1 & 1 \\ 1 & -1 \end{pmatrix}. \quad (1)$$

When the photon with a wave function $|\psi\rangle_i$ is directed to the MZI, BS_1 works as a divider to split the wave function into two sub-wave functions, namely, $|\psi\rangle_{in,1}$ and $|\psi\rangle_{in,2}$, traveling along path₁ and path₂. This is described by

$$\begin{pmatrix} |\psi\rangle_{in,1} \\ |\psi\rangle_{in,2} \end{pmatrix} = H \begin{pmatrix} |\psi\rangle_i \\ 0 \end{pmatrix}, \quad (2)$$

directly resulting in $|\psi\rangle_{in,1} = |\psi\rangle_{in,2} = |\psi\rangle_i / \sqrt{2}$. After a phase shifter ϕ , an additional phase $e^{i\phi}$ is introduced and $|\psi\rangle_{in,1}$ becomes $e^{i\phi}|\psi\rangle_{in,1}$. If BS_2 is absent, then the two sub-wave functions are directed to the detectors D_1 and D_2 , without the interference between them. The detection probabilities of D_1 and D_2 are $P_1 = {}_{in,1} \langle \psi | \psi \rangle_{in,1} = 1/2$ and $P_2 = {}_{in,2} \langle \psi | \psi \rangle_{in,2} = 1/2$, respectively. The sub-waves exist at both arms, and there is an equal probability that the photon collapses in either detectors. When a click is registered in D_1 (D_2), both sub-wave functions collapse to D_1 (D_2) instantly. In the standard interpretation, this open MZI is usually interpreted as showing the particle nature, wherein the photon chooses only a single arm to travel. In contrast, the REIN interprets it in such a way that the photon still travels along both arms simultaneously. The wave function of the photon, which is the photon itself, travels along both arms. The reason why they do not interfere is that the sub-waves along the two arms do not encounter each other, and both them arrive at the two detectors. According to the measurement postulate of quantum mechanics, the measurement result will be one of the eigenstates, in this case, the discrete positions of D_1 and D_2 , with some probabilities.

If BS_2 is present, the coalescence of the two sub-waves occurs, forming the two new sub-waves $|\psi\rangle_{out,1}$ and $|\psi\rangle_{out,2}$, which are directed to D_1 and D_2 , respectively. After the transformation of BS_2 , we have

$$|\psi\rangle_{out,1} = \frac{1}{\sqrt{2}} (e^{i\phi} |\psi\rangle_{in,1} - |\psi\rangle_{in,2}), \quad (3)$$

and

$$|\psi\rangle_{out,2} = \frac{1}{\sqrt{2}} (e^{i\phi} |\psi\rangle_{in,1} + |\psi\rangle_{in,2}). \quad (4)$$

The detection probabilities of D_1 and D_2 are given by $P_1 = {}_{out,1} \langle \psi | \psi \rangle_{out,1} = \sin^2 \frac{\phi}{2}$ and $P_2 = {}_{out,2} \langle \psi | \psi \rangle_{out,2} = \cos^2 \frac{\phi}{2}$. As ϕ varies, an interference pattern appears. This has been used to show a wave behavior in the closed MZI setting experiment. However, in the REIN perspective, the quantum wave behaves exactly the same as that in the open MZI before reaching the end of the MZI. The insertion of BS_2 results in the encounter between two sub-waves and the interference due to their phases. Similar to the open MZI, when a click is registered in D_1 (D_2), both the output sub-waves collapse to D_1 (D_2) simultaneously. In the special case where $\phi = 0$, $|\psi\rangle_{in,1}$ and $|\psi\rangle_{in,2}$ interfere constructively to give $|\psi\rangle_{out,2} = |\psi\rangle_i$ along path₂, and interfere destructively to give $|\psi\rangle_{out,1} = 0$ along path₁. In this case, only D_2 can detect the photon.

If it is decided to insert BS_2 at the end of the MZI when the two sub-waves encounter each other, then $|\psi\rangle_{in,\rho}$ can be divided into two components and expressed as:

$$|\psi\rangle_{in,\rho} = |\psi\rangle_{in,\rho}^p + |\psi\rangle_{in,\rho}^w, \quad (5)$$

with $\rho = 1, 2$. Here, $|\psi\rangle_{in,\rho}^p$ is a part of the sub-wave, which has passed the exit point when BS₂ is decided to be inserted, and $|\psi\rangle_{in,\rho}^w$ is the remaining part, which is subject to the action of BS₂. The interference between $|\psi\rangle_{in,1}^w$ and $|\psi\rangle_{in,2}^w$ occurs because BS₂ is present when they leave MZI. After the second beam splitter, it gives

$$|\psi\rangle_{out,1}^w = \frac{1}{\sqrt{2}}(e^{i\phi}|\psi\rangle_{in,1}^w - |\psi\rangle_{in,2}^w), \quad (6)$$

and

$$|\psi\rangle_{out,2}^w = \frac{1}{\sqrt{2}}(e^{i\phi}|\psi\rangle_{in,1}^w + |\psi\rangle_{in,2}^w), \quad (7)$$

where $|\psi\rangle_{out,\rho}^w$ is the component of $|\psi\rangle_{out,\rho}$ which gives the wave behavior in the standard interpretation. The interference between $|\psi\rangle_{in,1}^p$ and $|\psi\rangle_{in,2}^p$ never occurs because BS₂ is absent when they exit out of the MZI. They are directed to the detectors along their paths. Therefore, we have

$$|\psi\rangle_{out,1}^p = e^{i\phi}|\psi\rangle_{in,1}^p, \quad (8)$$

and

$$|\psi\rangle_{out,2}^p = |\psi\rangle_{in,2}^p, \quad (9)$$

where $|\psi\rangle_{out,\rho}^p$ is the component of $|\psi\rangle_{out,\rho}$ that gives the particle behavior in the standard interpretation. Combining eqs. (6)-(9), we have the two new sub-waves after the action of BS₂:

$$|\psi\rangle_{out,1} = |\psi\rangle_{out,1}^p + \frac{1}{\sqrt{2}}(e^{i\phi}|\psi\rangle_{in,1}^w - |\psi\rangle_{in,2}^w), \quad (10)$$

and

$$|\psi\rangle_{out,2} = |\psi\rangle_{out,2}^p + \frac{1}{\sqrt{2}}(e^{i\phi}|\psi\rangle_{in,1}^w + |\psi\rangle_{in,2}^w). \quad (11)$$

Ensuring the two paths inside the MZI are of equal length, we have $|\psi\rangle_{in,1}^p = |\psi\rangle_{in,2}^p$ and $|\psi\rangle_{in,1}^w = |\psi\rangle_{in,2}^w$. The detection probabilities of D₁ and D₂ are respectively expressed as:

$$P_1 = 2 \sin^2 \frac{\phi}{2} P_1^w + P_1^p, \quad (12)$$

and

$$P_2 = 2 \cos^2 \frac{\phi}{2} P_2^w + P_2^p. \quad (13)$$

Here the relation

$$P_{in,\rho}^p \{|\psi\rangle_{in,\rho}^w\} = 0 \quad (14)$$

is employed, and $P_{in,\rho}^w = \langle \psi | \psi \rangle_{in,\rho}^w$ ($P_{in,\rho}^p = \langle \psi | \psi \rangle_{in,\rho}^p$) is the probability that could (could not) show the interference behavior in the ρ -th arm. They satisfy

$$P_{in,\rho}^p + P_{in,\rho}^w = 1. \quad (15)$$

Apparently, $P_1^w = P_2^w = P_w/2$ and $P_1^p = P_2^p = P_p/2$, where P_w (P_p) is the total probability that will show (not show) the interference (which is called wave (particle) nature in standard interpretation). Thus, we have

$$P_1 = \sin^2 \frac{\phi}{2} + \frac{\cos \phi}{2} P_p, \quad (16)$$

and

$$P_2 = \cos^2 \frac{\phi}{2} - \frac{\cos \phi}{2} P_p, \quad (17)$$

and $P_1 + P_2 = 1$. In the special case where $\phi = 0$, BS₂ is inserted when half of the two sub-waves have exited the MZI, this results in $P_1 = 1/4$ and $P_2 = 3/4$. P_1 and P_2 as functions of the phase ϕ at several fixed values of P_p are shown in Figure 2. As can be seen in the figure, P_p changes from 0.0 to 1.0 and the detection probabilities at the two arms change from a complete interference pattern to a flat line that exhibits no interference. In the standard interpretation, the photon behavior changes from a wave to a particle. When the value of P_p is fixed at a value between the two extremes, the probabilities are the incoherent superposition of a flat line and an interference pattern. In the standard interpretation, a single photon simultaneously exhibits a wave nature and a particle nature.

This is equivalent to the QDC experiment, wherein the controlled-insertion of the second beam splitter serves as a controlled unitary gate that produces the superposed quantum state. The position of insertion gives the form of the unitary gate. At the middle point insertion, the controlled gate is a Hadamard gate. This can also be explained in terms of the duality quantum computing framework in refs. [27-29], as in ref. [12].

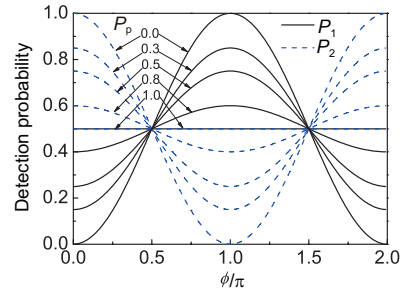


Figure 2 (Color online) The detection probabilities, P_1 and P_2 , as functions of the phase ϕ at fixed values of P_p . P_p can be controlled by the BS₂ insertion instant of time, which divides the passing sub-waves into different ratios between particle-like and wave-like parts. When $P_p = 1.0$, BS₂ is not inserted, no interference occurs and the photon exhibits particle-like nature. When $P_p = 0$, BS₂ is inserted before the sub-waves arrive at the exit point, full interference occurs, and the photon shows a wave-like behavior. In between these two extremes, photons simultaneously exhibit a partial particle-like nature and partial wave-like nature as in the QDC case.

4 The EDC experiment

We design and implement the EDC experiment, in which the insertion of the output beam splitter is decided at the end of the MZI when the photon is passing through the exit point. The experimental setup is shown in Figure 3. The experiment starts from a 780 nm continuous-wave polarized laser (SWL) with a linewidth of 600 kHz. The first EOM₁ modulates and transforms the continuous light into pulse sequences, which are then attenuated to the single-photon level by using an attenuator. Then, the pulses are sent into the MZI, which is composed of two 50/50 beam splitters and two reflection mirrors. The input beam splitter (BS₁) divides the wave function of the single photon into two spatially separated components of equal amplitude, and the output beams splitter (BS₂) works as a combiner of the two components.

The two arms of the MZI are of equal length. The insertion of BS₂ is realized by using two additional modulators (EOM₂ and EOM₃) that are inserted in the two arms of the MZI, which are of equal distance from the input BS₁. The half-wave voltages of the three modulators are $V_\pi = (91 \pm 1)$ V. When the TTL (transistor-transistor logic) signal is the “high” voltage level, the half-wave voltage applies to the EOM and the photon is transmitted, that is, the beam splitter is lifted. Otherwise, the photon is reflected by the EOM, and the beam splitter is inserted.

Three TTL control signals with a repetition rate of 1 MHz determine whether or not the half-wave voltages apply to the three modulators. EOM₁ is used to cut the continuous waves into fragmented pulses at the single photon level as mentioned above. The two modulators, EOM₂ and EOM₃, are

used to split the two sub-waves of the single photon into four sub-waves. When EOM₂ and EOM₃ are in the high-voltage level, the two photon sub-waves are transmitted, and the MZI is open. The sub-waves are directed to the detectors D₃ and D₄, respectively, and manifest a particle-like behavior. When the TTL is in the low-voltage level, two of the sub-waves are reflected and pass through the output BS₂. Their paths are indistinguishable, and hence, interfere with each other. The MZI is closed for them, hence, they show a wave-like behavior in the standard delayed-choice interpretation.

By maintaining the control signals S₂ and S₃ in-phase so that they act as a single one, we can tune the time difference t_d between the signal S₁ and S₂ to decide the insertion time of BS₂. t_d is the insertion time, namely, $t_d/(T/2)$ parts of the sub-wave have transmitted, and move toward detectors D₃ and D₄, where $T/2$ is the length of the pulse. The relative detection probability of D₃ is given by

$$\begin{aligned} R_p &= \frac{P_{\text{out},1}^p \{|\psi\rangle\}_{\text{out},1}^p}{P_{\text{out},1}^p \{|\psi\rangle\}_{\text{out},1}^p + P_{\text{out},2}^p \{|\psi\rangle\}_{\text{out},2}^p} \\ &= \frac{P_1^p}{P_1^p + P_2^p} = \frac{N_3}{N_3 + N_4} \\ &= \frac{1}{2}, \end{aligned} \quad (18)$$

where N_3 and N_4 are the number of clicks registered by detectors D₃ and D₄, respectively. The result is independent of t_d , which is interpreted as exhibiting a particle-like nature in the standard interpretation. In the REIN, this is naturally explained by the non-interfering sub-waves traveling through both arms simultaneously. The detection by either D₃ or D₄

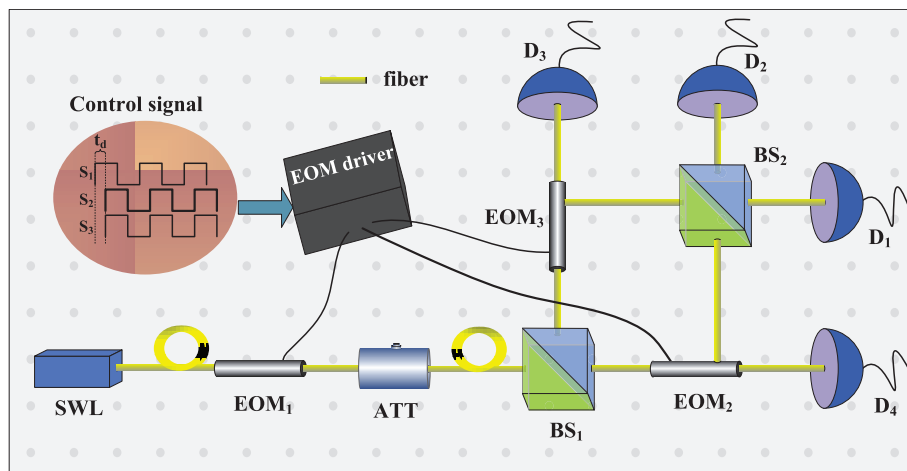


Figure 3 (Color online) Experimental realization of the EDC experiment. SWL: single-wavelength laser. EOM: electro-optic modulator. ATT: optical attenuator. BS: beam splitter. D: single photon detector. Single photons are produced by attenuating the pulses generated by EOM₁ from a continuous light wave emitted from a 780 nm laser with a linewidth of 600 kHz. The input and output beam splitters are of 50/50 in transmission and reflection. The square waves TTL S₂ and S₃ signals apply to the EOM₂ and EOM₃, respectively, which serve as a controller for insertion of the second beam splitter by guiding the sub-waves to different channels. The control signals S₂ and S₃ are in-phase, and t_d is the time difference between S₁ and S₂, S₃.

is due to the measurement, which gives equal probabilities to each of the detectors.

On the other hand, because of BS₂, the interference between the two sub-waves, $|\psi\rangle_{in,1}^w$ and $|\psi\rangle_{in,2}^w$, occurs. The two resulting sub-waves, $|\psi\rangle_{out,1}^w$ and $|\psi\rangle_{out,2}^w$, are then directed to detectors, D₁ and D₂, respectively. The relative detection probability of D₁ is evaluated as:

$$\begin{aligned} R_w &= \frac{w}{out,1} \{|\psi\rangle_{out,1}^w\} \\ &= P_1^w (1 - \cos \phi), \\ &= \frac{N_1}{N_t}, \end{aligned} \quad (19)$$

where N_1 is the number of clicks registered by detectors D₁, and $N_t = \sum_i^4 N_i$. By choosing $\phi = 0$, the result $R_w = 0$ shows that destructive interference leads to completely canceling each other in the output of D₁. P_w (P_p) is a probability that a single photon will (will not) show a wave (particle) nature,

$$\begin{aligned} P_w &= \frac{w}{out,1} \{|\psi\rangle_{out,1}^w\} + \frac{w}{out,2} \{|\psi\rangle_{out,2}^w\} \\ &= 2P_1^w \sin^2 \phi/2 + 2P_1^w \cos^2 \phi/2 \\ &= 2P_1^w = (N_1 + N_2)/N_t, \end{aligned} \quad (20)$$

and

$$\begin{aligned} P_p &= \frac{p}{out,1} \{|\psi\rangle_{out,1}^p\} + \frac{p}{out,2} \{|\psi\rangle_{out,2}^p\} \\ &= 2P_1^p = (N_3 + N_4)/N_t, \end{aligned} \quad (21)$$

with $N_t = \sum_i^4 N_i$ and $P_w + P_p = 1$.

In our experiment, photon uniformly distributes in a pulse, thereby yielding,

$$P_p = 2t_d/T, \quad (22)$$

and

$$P_w = 1 - P_p = 1 - 2t_d/T. \quad (23)$$

Both P_p and P_w are linearly dependent on the delayed time t_d .

The experimental results are shown in Figure 4. As can be seen, the wave function of a single photon is divided into 4 parts and detected by 4 detectors, respectively. If the output BS₂ is present, we observe the interference fringes with a tunable phase difference between the two paths, in which the single photon sub-waves travel. When the two arms of the interferometer are of equal length, the two paths are fully recombined by the output BS₂ and are perfectly indistinguishable. We observe a register, with probability 1, a click in only one of the two detectors (D₁ and D₂) placed on the output ports of the interferometer. If the output BS₂ is absent, each detector has 50% probability to register a click. In the

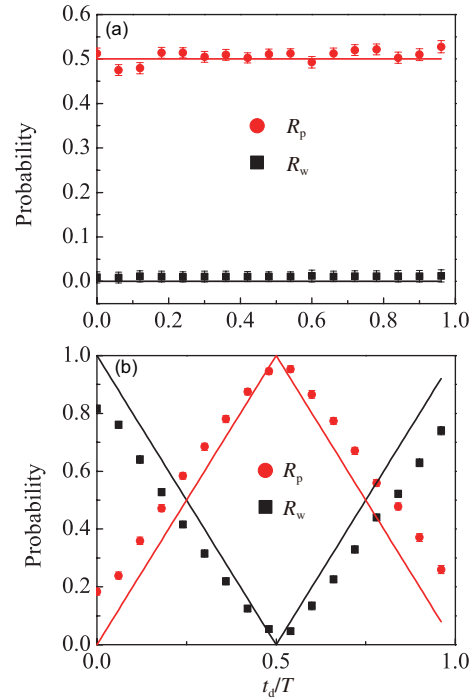


Figure 4 (Color online) Experimental results. (a) Black points represent ratio $R_w = N_1/(N_1 + N_2)$ and red points are $R_p = N_3/(N_3 + N_4)$, representing the wave-like behavior and particle-like behavior, respectively, in standard interpretation. (b) The total probability P_w of interfering photon (black dots) and P_p that of non-interfering photon (red dots).

standard interpretation, this is interpreted as the photon having a particle-like behavior, and the photon travels through a single path to one of the detectors. In the REIN view, these two cases are interpreted in a unified way. The open setting case is just like the closed setting case, and the only difference between them is whether or not BS₂ exists. Before the exit point, the sub-waves travel in both arms in both the open and closed settings. Without BS₂, the sub-waves travel without interference, whereas with BS₂, the sub-waves travel with interference, which may lead to the photon wave going to one detector completely.

As seen in Figure 4(a), the black points $R_w = N_1/(N_1 + N_2)$ show the wave-like behavior, and the red ones representing $R_p = N_3/(N_3 + N_4)$ show the particle-like behavior. P_w gives the percentage of the component of the single-photon wave function showing a wave-like behavior and P_p gives that of the component showing a particle-like behavior. The ratios P_w and P_p are allowed to vary between 0 and 1 when the time delay t_d varies between 0 and T , where T is the period of the control signal, $T/2$ are in the high-voltage level and $T/2$ are in the low-voltage level. The wave function of the single photon distributes with uniform intensity along the propagation direction due to the rectangular control signals with 50% duty cycle. Given that the frequency of the control signal, $f = 1/T$, is larger than the laser linewidth of 600 kHz, the

coherence length of the light modulated by EOM_1 approaches that of the pulse. In addition, the length of the single-photon wave function along the propagation direction could be considered as that of the pulse $L = Tc/(2n)$ with the light speed c and the effective refractive index n . Hence, the two quantities P_w and P_p change linearly with the time-delay t_d , as shown in Figure 4(b).

5 Discussion

In this work, we have presented the REIN of quantum mechanics. In the REIN, the wave function is the real existence of a quantum object. According to the REIN, a quantum object should not be considered as a rigid particle that is difficult to visualize in terms of how travels through both arms of an MZI simultaneously. Instead, it is natural to imagine that a quantum object travels through both arms as an extended, disjointed clouds of bodies as the wave function occupies and travels. It is not merely a mathematical description. Like a classical wave, a quantum wave can be divided into sub-waves, which in turn, can be recombined. When they are measured, they collapse and show a particle-like nature. The essential difference between a quantum wave and a classical wave is that the former collapses in totality, namely, the whole of the quantum wave, and whatever is scattered in space collapses into a single point instantly. Apart from this, a quantum wave can be viewed almost in the same manner as a classical wave.

Here we stress again the essential features of the REIN. In the REIN perspective, the photon sub-waves travel through both arms in the MZI. The simultaneous travel of a photon through the two arms is easy to comprehend and understand: the photon is no longer a ball-like particle; rather, it is an extended and even separated stuff distributed in space in the form of quantum wave. The sub-waves travel simultaneously along the two arms. Each sub-wave contains the full attributes of the quantum object: when measured, it collapses with some probability to exhibit the full properties of the quantum object, such as spins, masses, and so on.

In the REIN view, the wave- or particle-like nature, in the standard interpretation of a delayed-choice MZI, is simply the interference or non-interference of the sub-waves of the single photons. These photons are all sub-waves before they are detected. When they are detected, they collapse and cause a click in the detector which is viewed as a particle.

The REIN perspective has been exploited in the duality quantum computer [27]. The duality quantum computer uses the superpositions of quantum sub-waves, thus allowing the linear combinations of unitary operators as generalized quantum gates. The mathematical expressions have been con-

structed and developed [30-34]. Recently, a study reported that linear combinations of unitary operators are superior in simulating Hamiltonian systems compared with traditional formalism of products of unitary operators [35].

The REIN idea is demonstrated by an EDC experiment proposed in the present work. By inserting a beam splitter as the two sub-waves encounter each other, one is able to allow the part of the sub-waves to interfere and the other part not to interfere, hence exhibiting the so-called wave-like nature and particle-like nature simultaneously, as in the QDC experiments. We have experimentally demonstrated the EDC proposal, and the experiment results support the REIN idea.

Note: This manuscript was first put in the Los-Alamos eprint server in 15 October 2014 as arXiv: 1410.4129. It is almost three years by now. It is worth noting that a recent experiment work by Zhou et al. [36] also confirms the real existence of quantum wave function. It has been shown that the precision-improved quantum simulation algorithm of Berry et al. [37] and the Childs-Wiebe quantum simulation algorithms are all duality quantum algorithms [38]. Duality quantum simulation algorithm for open quantum systems is reported in ref. [39], and it has the advantage of being more efficient and with higher precision. The quantum algorithm for solving a set of linear equations [40] is also a duality quantum algorithm [41]. Duality quantum computing can also be used in other related studies [42, 43].

This work was supported by the National Natural Science Foundation of China (Grants No. 11474181), the National Basic Research Program of China (Grant No. 2011CB9216002), and the Open Research Fund Program of the State Key Laboratory of Low-Dimensional Quantum Physics, Tsinghua University.

Open Access This article is distributed under the terms of the Creative Commons Attribution 4.0 International License (<http://creativecommons.org/licenses/by/4.0/>), which permits use, duplication, adaptation, distribution and reproduction in any medium or format, as long as you give appropriate credit to the original author(s) and the source, provide a link to the Creative Commons license and indicate if changes were made.

- 1 K. F. Weizsäcker, *Z. Phys.* **70**, 114 (1931).
- 2 C. F. von Weizsäcker, *Z. Phys.* **118**, 489 (1941).
- 3 J. A. Wheeler, in: *Mathematical Foundations of Quantum Theory*, edited by A. R. Marlow (Academic Press, Cambridge, 1978), pp. 9-48.
- 4 T. Hellmuth, H. Walther, A. Zajonc, and W. Schleich, *Phys. Rev. A* **35**, 2532 (1987).
- 5 B. J. Lawson-Daku, R. Asimov, O. Gorceix, C. Miniatura, J. Robert, and J. Baudon, *Phys. Rev. A* **54**, 5042 (1996).
- 6 Y. H. Kim, R. Yu, S. P. Kulik, Y. Shih, and M. O. Scully, *Phys. Rev. Lett.* **84**, 1 (2000).
- 7 V. Jacques, E. Wu, F. Grosshans, F. Treussart, P. Grangier, A. Aspect, and J. F. Roch, *Science* **315**, 966 (2007).
- 8 V. Jacques, E. Wu, F. Grosshans, F. Treussart, P. Grangier, A. Aspect, and J. F. Roch, *Phys. Rev. Lett.* **100**, 220402 (2008).

- 9 X. Ma, S. Zotter, J. Kofler, R. Ursin, T. Jennewein, Brukner, and A. Zeilinger, *Nat. Phys.* **8**, 480 (2012).
- 10 R. Ionicioiu, and D. R. Terno, *Phys. Rev. Lett.* **107**, 230406 (2011).
- 11 M. Schirber, *Physics* **4**, 102 (2011).
- 12 S. S. Roy, A. Shukla, and T. S. Mahesh, *Phys. Rev. A* **85**, 022109 (2012).
- 13 R. Auccaise, R. M. Serra, J. G. Filgueiras, R. S. Sarthour, I. S. Oliveira, and L. C. Céleri, *Phys. Rev. A* **85**, 032121 (2012).
- 14 A. Peruzzo, P. Shadbolt, N. Brunner, S. Popescu, and J. L. O'Brien, *Science* **338**, 634 (2012).
- 15 F. Kaiser, T. Coudreau, P. Milman, D. B. Ostrowsky, and S. Tanzilli, *Science* **338**, 637 (2012).
- 16 J. S. Tang, Y. L. Li, X. Y. Xu, G. Y. Xiang, C. F. Li, and G. C. Guo, *Nat. Photon.* **6**, 602 (2012).
- 17 G. Adesso, and D. Girolami, *Nat. Photon.* **6**, 579 (2012).
- 18 L. C. Céleri, R. M. Gomes, R. Ionicioiu, T. Jennewein, R. B. Mann, and D. R. Terno, *Found. Phys.* **44**, 576 (2014).
- 19 R. Ionicioiu, T. Jennewein, R. B. Mann, and D. R. Terno, *Nat. Commun.* **5**, 3997 (2014).
- 20 J. S. Lundeen, B. Sutherland, A. Patel, C. Stewart, and C. Bamber, *Nature* **474**, 188 (2011).
- 21 S. Kocsis, B. Braverman, S. Ravets, M. J. Stevens, R. P. Mirin, L. K. Shalm, and A. M. Steinberg, *Science* **332**, 1170 (2011).
- 22 W. P. Schleich, M. Freyberger, and M. S. Zubairy, *Phys. Rev. A* **87**, 014102 (2013).
- 23 L. D. Landau, and E. M. Lifshitz, *Quantum Mechanics: Non-Relativistic Theory in Course of Theoretical Physics Vol. 3*, 3rd ed, (Pergamon Press, Oxford, 1989), p. 6.
- 24 C. Cohen-Tannoudji, B. Diu, and F. Laloe, *Quantum Mechanics Vol. 1* (Wiley-Interscience, New York, 2006), p. 19.
- 25 N. D. Mermin, *Phys. Today* **62**, 8 (2009).
- 26 G. L. Long, *Sci. Bull.* **62**, 1355 (2017).
- 27 G. L. Long, *Commun. Theor. Phys.* **45**, 825 (2006).
- 28 G. L. Long, and L. Yang, *Commun. Theor. Phys.* **50**, 1303 (2008).
- 29 G. L. Long, L. Yang, and W. Chuan, *Commun. Theor. Phys.* **51**, 65 (2009).
- 30 S. Gudder, *Quant. Inf. Process.* **6**, 37 (2007).
- 31 G. L. Long, *Quant. Inf. Process.* **6**, 49 (2007).
- 32 G. L. Long, and L. Yang, *Commun. Theor. Phys.* **50**, 1303 (2008).
- 33 G. L. Long, *Int. J. Theor. Phys.* **50**, 1305 (2011).
- 34 C. Y. Li, W. Y. Wang, C. Wang, S.Y. Song, and G. L. Long, in: *Duality Quantum Information and Duality Quantum Communication: Proceedings of the International Conference on Advances in Quantum Theory*, edited by G. Jaeger, A. Khrennikov, M. Schlosshauer, and G. Weihs (AIP Publishing, Växjö, 2011) pp. 158-165.
- 35 A. M. Childs, and N. Wiebe, arXiv: [1202.5822](https://arxiv.org/abs/1202.5822).
- 36 Z. Y. Zhou, Z. H. Zhu, S. L. Liu, Y. H. Li, S. Shi, D. S. Ding, L. X. Chen, W. Gao, G. C. Guo, and B. S. Shi, *Sci. Bull.* **62**, 1185 (2017).
- 37 D. W. Berry, A. M. Childs, R. Cleve, R. Kothari, and R. D. Somma, *Phys. Rev. Lett.* **114**, 090502 (2015).
- 38 S. J. Wei, and G. L. Long, *Quant. Inf. Process.* **15**, 1189 (2016).
- 39 S. J. Wei, D. Ruan, and G. L. Long, *Sci. Rep.* **6**, 30727 (2016).
- 40 A. W. Harrow, A. Hassidim, and S. Lloyd, *Phys. Rev. Lett.* **103**, 150502 (2009).
- 41 S. J. Wei, Z. R. Zou, D. Ruan, and G. L. Long, in *Realization of the Algorithm for System of Linear Equations in Duality Quantum Computing: Proceeding of IEEE 85th Vehicular Technology Conference* (Spring, Sydney, 2017).
- 42 X. Qiang, X. Zhou, K. Aungskunsiri, H. Cable, and J. L. O'Brien, *Quant. Sci. Technol.* **2**, 045002 (2017).
- 43 R. J. Marshman, A. P. Lund, P. P. Rohde, and T. C. Ralph, arXiv: [1709.02157](https://arxiv.org/abs/1709.02157).